Available online at www.sciencedirect.com
SCIENCE DIRECT®

ELSEVIER

Journal of Sound and Vibration 288 (2005) 931–955

JOURNAL OF SOUND AND VIBRATION

www.elsevier.com/locate/jsvi

Free vibration analysis of orthotropic rectangular plates with variable thickness and general boundary conditions

M. Huang[a,*], X.Q. Ma[b], T. Sakiyama[a], H. Matuda[a], C. Morita[a]

[a]*Department of Structural Engineering, Nagasaki University, Nagasaki 852, Japan*
[b]*Department of Mechanical Engineering, Yanshan University, PR China*

Received 25 June 2003; received in revised form 19 October 2004; accepted 13 January 2005
Available online 9 June 2005

Abstract

A discrete method is developed for analyzing the free vibration problem of orthotropic rectangular plates with variable thickness. The Green function, which is obtained by transforming the differential equations into integral equations and using numerical integration, is used to establish the characteristic equation of the free vibration. The effects of the aspect ratios, boundary conditions, the variation of the thickness on the frequencies are considered. By comparing the numerical results obtained by the present method with the those previously published, the efficiency and accuracy of the present method are investigated. The frequency parameters are obtained for the orthotropic plates with general boundary conditions and variable thickness in one or two directions. The model shapes are given for some of the square plates with three kinds of thickness variations.

1. Introduction

Structural components, such as plates with variable thickness, are widely used in aeronautical, mechanical and ocean structures. The variable thickness is used to alter resonant frequency and to

*Corresponding author. Tel.: +81 95 819 2592.
E-mail address: huang@st.nagasaki-u.ac.jp (M. Huang).

0022-460X/$ - see front matter
doi:10.1016/j.jsv.2005.01.052

reduce the size and weight of the structure. Therefore, the vibration analysis of the plates with variable thickness is an important topic for the researchers. Bhat et al. [1] used four kinds of methods to obtain natural frequencies of isotropic rectangular plates with linearly variable thickness in one direction. A comparison of the results of the four methods was given. Roy and Ganesan [2] investigated the dynamic response of an isotropic square plate with linear or parabolic thickness variation in one direction. The effects of thickness variation on natural frequencies, dynamic displacements and stresses were considered. The Rayleigh–Ritz method was used to study the free vibration of isotropic rectangular plates with variable thickness in two directions by Singh and Saxena [3]. Liew and Lim [4] analyzed the free vibration of isotropic trapezoidal plates with variable thickness. They also analyzed the free vibration of isotropic doubly-tapered rectangular plates [5]. The Rayleigh–Ritz method was employed. The first eight frequencies were presented for plates with six kinds of boundary conditions and various aspect ratios. Liew et al. [6] presented a semi-analytical method to analyze the free vibration of isotropic rectangular plates with abrupt thickness variation in the central part. The frequency parameters and mode shapes were given for three boundary conditions. A lots of papers have been republished on the subject of the free vibration of isotropic plates with variable thickness and some of them were well compiled in Ref. [7]. The situation pertaining to orthotropic plates with variable thickness is quite different. Although orthotropic plates have received more and more attention due to their unique advantages such as high strength-to-weigh ratio, high stiffness-to-weigh ratio and low density, only a few papers have been reported about the free vibration of those plates. Sakata [8] utilized the double trigonometric series to obtain the characteristic equation of a clamped orthotropic rectangular plate with linearly varying thickness in one direction. The effects of aspect ratios and flexural rigidity on fundamental frequency were evaluated. Malhotra et al. [9] investigated the vibrations of orthotropic square plates with parabolic thickness variation in one direction. Rayleigh–Ritz method was used to obtain fundamental frequencies for four boundary conditions. Bambill et al. [10] used the Rayleigh–Ritz method and the finite element method to analyze the transverse vibration of an orthotropic rectangular plate with linearly varying thickness in one direction. Fundamental frequencies were presented for plates with a free edge.Bert and Malik [11] adopted a semi-analytical approach in the differential quadrature method to investigate free vibration of isotropic and orthotropic rectangular plates with linearly varying thickness in one direction. They realized the information published on tapered orthotropic plates was very scant and they presented a number of numerical results for plates with two opposite edges simply supported. Ashour [12] studied the flexural vibration of orthotropic plates with variable thickness in one direction by employing the finite strip transition matrix technique. The frequencies were obtained for plates with two opposite edges having the same boundary conditions and the same thickness. But the boundary conditions of the two opposite edges were no longer restricted to simply supported conditions. Although the results obtained by Ashour were accurate enough for some boundary conditions, for the other boundary conditions, some of the frequency parameters, even the fundamental frequency parameter, seemed to be lost. The scantiness of the information about the free vibration problem of the orthotropic plates with variable thickness, especially for the orthotropic plates with general boundary conditions and variable thickness in two directions, motivates the authors to do the present work.

In this paper, a discrete method is used to analyze the free vibration of orthotropic rectangular plates with variable thickness. The method was proposed by some of the authors. It has been used to solve the free vibration problems of tapered isotropic plates with three kinds of boundary conditions [13] and simply supported orthotropic square plate with a hole [14]. No prior assumption of shape of deflection, such as shape function used in Rayleigh–Ritz method, is needed in the proposed method. The fundamental differential equations involving Dirac's delta functions are established and satisfied exactly throughout the whole plate. By transforming these equations into integral equations and using numerical integration, the solutions are obtained at the discrete points. The Green function, which is the solution for deflection, is used to obtain the characteristic equation of the free vibration. The convergent results are obtained by using Richardson's extrapolation formula for two cases of suitably smaller divisional numbers. The purpose of the paper is to (1) investigate the efficiency and accuracy of the present method for the free vibration problem of tapered orthotropic rectangular plates with general boundary conditions, (2) discuss the effects of the boundary conditions, the aspect ratio and variable thickness on the frequency parameter, and (3) give some new data and mode shapes for the plates with general boundary condition and variable thickness in one or two directions.

2. Fundamental differential equations

An xyz coordinate system is used in the present study with its x–y plane contained in middle plane of an orthotropic rectangular plate and the z-axis perpendicular to the middle plane of the plate. The thickness, the length and the width of the orthotropic rectangular plate are h, a and b, respectively. The principle material axes of the plate in the longitudinal, transverse and normal directions are designated as 1, 2 and 3.

The displacements u, v and w in the x, y and z directions are assumed to be

$$u = z\theta_x(x,y), \quad v = z\theta_y(x,y), \quad w = w(x,y), \tag{1}$$

where $\theta_x(x,y)$ and $\theta_y(x,y)$ are the rotations in the x–z and y–z planes.

For small displacements, the strain–displacement relations of elasticity yield

$$\begin{bmatrix} \varepsilon_x \\ \varepsilon_y \\ \gamma_{xy} \\ \gamma_{yz} \\ \gamma_{xz} \end{bmatrix} = \begin{bmatrix} z\dfrac{\partial \theta_x}{\partial x} \\ zd\dfrac{\partial \theta_y}{\partial y} \\ z\left(d\dfrac{\partial \theta_x}{\partial y} + \dfrac{\partial \theta_y}{\partial x}\right) \\ \dfrac{\partial w}{\partial y} + \theta_y \\ \dfrac{\partial w}{\partial x} + \theta_x \end{bmatrix}. \tag{2}$$

For orthotropic plates, the stress–strain relations can be expressed as

$$\begin{bmatrix} \sigma_x \\ \sigma_y \\ \tau_{xy} \\ \tau_{yz} \\ \tau_{xz} \end{bmatrix} = \begin{bmatrix} \bar{Q}_{11} & \bar{Q}_{12} & 0 & 0 & 0 \\ \bar{Q}_{12} & \bar{Q}_{22} & 0 & 0 & 0 \\ 0 & 0 & \bar{Q}_{66} & 0 & 0 \\ 0 & 0 & 0 & \bar{Q}_{44} & 0 \\ 0 & 0 & 0 & 0 & \bar{Q}_{55} \end{bmatrix} \begin{bmatrix} \varepsilon_x \\ \varepsilon_y \\ \gamma_{xy} \\ \gamma_{yz} \\ \gamma_{xz} \end{bmatrix}, \tag{3}$$

where $\bar{Q}_{11} = E_1/(1 - v_{12}v_{21})$, $\bar{Q}_{12} = v_{12}E_2/(1 - v_{12}v_{21})$, $\bar{Q}_{22} = E_2/(1 - v_{12}v_{21})$, $\bar{Q}_{66} = G_{12}$, $\bar{Q}_{44} = G_{23}$, $\bar{Q}_{55} = G_{13}$. E_1 is the axial modulus in the 1-direction, E_2 is the axial modulus in the 2-direction, v_{12} is the Poisson's ratio associated with loading in the 1-direction and strain in the 2-direction, v_{21} is the Poisson's ratio associated with loading in the 2-direction and strain in the 1-direction, G_{23}, G_{13} and G_{12} are the shear moduli in 2–3, 1–3 and 1–2 planes.

The moments and the shear forces can be given by

$$\begin{aligned} M_x &= \int_{-h/2}^{h/2} \sigma_x z \,\mathrm{d}z, \quad M_y = \int_{-h/2}^{h/2} \sigma_y z \,\mathrm{d}z, \quad M_{xy} = \int_{-h/2}^{h/2} \sigma_{xy} z \,\mathrm{d}z, \\ Q_y &= \int_{-h/2}^{h/2} \tau_{yz} \,\mathrm{d}z, \quad Q_x = \int_{-h/2}^{h/2} \tau_{xz} \,\mathrm{d}z. \end{aligned} \tag{4}$$

By using Eqs. (2)–(4), the relations of the moment–displacement and the shear force–displacement can be obtained as

$$\begin{bmatrix} M_x \\ M_y \\ M_{xy} \\ Q_y \\ Q_x \end{bmatrix} = \begin{bmatrix} D_{11} & D_{12} & 0 & 0 & 0 \\ D_{12} & D_{22} & 0 & 0 & 0 \\ 0 & 0 & D_{66} & 0 & 0 \\ 0 & 0 & 0 & A_{44} & 0 \\ 0 & 0 & 0 & 0 & A_{55} \end{bmatrix} \begin{bmatrix} \dfrac{\partial \theta_x}{\partial x} \\ \dfrac{\partial \theta_y}{\partial y} \\ \dfrac{\partial \theta_x}{\partial y} + \dfrac{\partial \theta_y}{\partial x} \\ \dfrac{\partial w}{\partial y} + \theta_y \\ \dfrac{\partial w}{\partial x} + \theta_x \end{bmatrix}, \tag{5}$$

where the extensional stiffness $A_{ij} = \bar{Q}_{ij}h$ $(i,j = 4, 5)$ and the bending stiffness $D_{ij} = \bar{Q}_{ij}h^3/12$ $(i,j = 1, 2, 6)$.

By using the non-dimensional expressions,

$$\begin{aligned} &[X_1, X_2] = \frac{a^2}{D_0(1 - v_{12}v_{21})}[Q_y, Q_x], \quad [X_3, X_4, X_5] = \frac{a}{D_0(1 - v_{12}v_{21})}[M_{xy}, M_y, M_x], \\ &[X_6, X_7, X_8] = \left[\theta_y, \theta_x, \frac{w}{a}\right], \quad [\eta, \zeta, \xi] = \left[\frac{x}{a}, \frac{y}{b}, \frac{z}{h}\right] \end{aligned}$$

the differential equations of the plate with a concentrated load $\bar{P}$ at point (x_q, y_r) are established as follows:

$$
\begin{aligned}
&\mu\frac{\partial X_2}{\partial \eta}+\frac{\partial X_1}{\partial \zeta}=-P\delta(\eta-\eta_q)\delta(\zeta-\zeta_r),\\
&\mu\frac{\partial X_3}{\partial \eta}+\frac{\partial X_4}{\partial \zeta}-\mu X_1=0,\\
&\mu\frac{\partial X_5}{\partial \eta}+\frac{\partial X_3}{\partial \zeta}-\mu X_2=0,\\
&\bar{D}_{11}\mu\frac{\partial X_7}{\partial \eta}+\bar{D}_{12}\frac{\partial X_6}{\partial \zeta}-\mu\bar{D}X_5=0,\\
&\bar{D}_{12}\mu\frac{\partial X_7}{\partial \eta}+\bar{D}_{22}\frac{\partial X_6}{\partial \zeta}-\mu\bar{D}X_4=0,\\
&\bar{D}_{66}\left(\frac{\partial X_7}{\partial \zeta}+\mu\frac{\partial X_6}{\partial \eta}\right)-\mu\bar{D}X_3=0,\\
&k\bar{A}_{44}\left(\frac{\partial X_8}{\partial \zeta}+\mu X_6\right)-\mu\overline{DT}X_1=0,\\
&\mu k\bar{A}_{55}\left(\frac{\partial X_8}{\partial \eta}+X_7\right)-\mu\overline{DT}X_2=0,
\end{aligned} \tag{6}
$$

where $P=\bar{P}a/(D_0(1-\nu_{12}\nu_{21}))$, $\bar{D}_{ij}=\bar{Q}_{ij}/E_2$, $\bar{D}=(h_0/h)^3$, $\bar{A}_{ij}=12(a/h_0)^2(\bar{Q}_{ij}/E_2)$, $\overline{DT}=h_0/h$, $D_0=E_2h_0^3/(12(1-\nu_{12}\nu_{21}))$ is the standard bending rigidity, h_0 is the standard thickness of the plate, $k=\frac{5}{6}$ is the shear correction factor, $\delta(\eta-\eta_q)$ and $\delta(\zeta-\zeta_r)$ are Dirac's delta functions.

In the above equation, the variable quantity h_0/h has been separated and expressed only in the quantities $\bar{D}$ and $\overline{DT}$ so that the equation can be used for the orthotropic plate with variable thickness. Eq. (6) can also be expressed as the following simple form.

$$\sum_{s=1}^{8}\left\{F_{1ts}\frac{\partial X_s}{\partial \zeta}+F_{2ts}\frac{\partial X_s}{\partial \eta}+F_{3ts}X_s\right\}+P\delta(\eta-\eta_q)\delta(\zeta-\zeta_r)\delta_{1t}=0 \quad (t=1\text{--}8), \tag{7}$$

where δ_{1t} is Kronecker's delta, $F_{111}=F_{123}=F_{134}=1$, $F_{146}=\bar{D}_{12}$, $F_{156}=\bar{D}_{22}$, $F_{167}=\bar{D}_{66}$, $F_{178}=k\bar{A}_{44}$, $F_{212}=F_{223}=F_{235}=\mu$, $F_{247}=\mu\bar{D}_{11}$, $F_{257}=\mu\bar{D}_{12}$, $F_{266}=\mu\bar{D}_{66}$, $F_{288}=\mu k\bar{A}_{55}$, $F_{321}=F_{332}=-\mu$, $F_{345}=F_{354}=F_{363}=-\mu\bar{D}$, $F_{371}=F_{382}=-\mu\overline{DT}$, $F_{376}=\mu k\bar{A}_{44}$, $F_{387}=\mu k\bar{A}_{55}$, other $F_{kts}=0$.

3. Discrete Green function

By dividing a rectangular plate vertically into m equal-length parts and horizontally into n equal-length parts as shown in Fig. 1, the plate can be considered as a group of discrete points which are the intersections of the $(m+1)$-vertical and $(n+1)$-horizontal dividing lines. To describe the present method conveniently, the rectangular area, $0\leqslant\eta\leqslant\eta_i$, $0\leqslant\zeta\leqslant\zeta_j$, corresponding to the arbitrary intersection (i,j) as shown in Fig. 1 is denoted as the area $[i,j]$, the intersection (i,j)

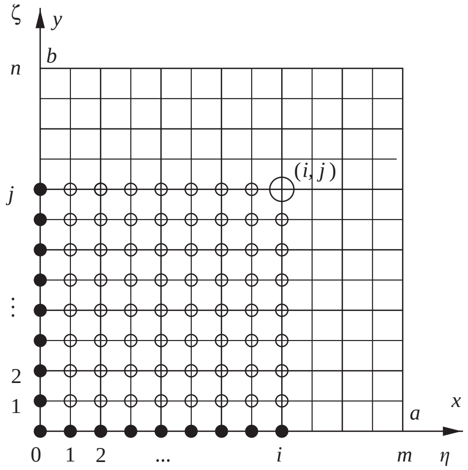

Fig. 1. Discrete points on a rectangular plate.

denoted by ◯ is called the main point of the area $[i,j]$, the intersections denoted by ∘ are called the inner-dependent points of the area, and the intersections denoted by • are called the boundary-dependent points of the area.

By integrating Eq. (7) over the area $[i,j]$, the following integral equation is obtained:

$$\sum_{s=1}^{8}\left\{F_{1ts}\int_0^{\eta_i}[X_s(\eta,\zeta_j)-X_s(\eta,0)]\,\mathrm{d}\eta+F_{2ts}\int_0^{\zeta_j}[X_s(\eta_i,\zeta)-X_s(0,\zeta)]\,\mathrm{d}\zeta\right.$$
$$\left.+F_{3ts}\int_0^{\eta_i}\int_0^{\zeta_j}X_s(\eta,\zeta)\,\mathrm{d}\eta\,\mathrm{d}\zeta\right\}+Pu(\eta-\eta_q)u(\zeta-\zeta_r)\delta_{1t}=0, \tag{8}$$

where $u(\eta-\eta_q)$ and $u(\zeta-\zeta_r)$ are the unit step functions.

Next, by applying the numerical integration method, the simultaneous equation for the unknown quantities $X_{sij}=X_s(\eta_i,\zeta_j)$ at the main point (i,j) of the area $[i,j]$ is obtained as follows:

$$\sum_{s=1}^{8}\left\{F_{1ts}\sum_{k=0}^{i}\beta_{ik}(X_{skj}-X_{sk0})+F_{2ts}\sum_{l=0}^{j}\beta_{jl}(X_{sil}-X_{s0l})\right.$$
$$\left.+F_{3ts}\sum_{k=0}^{i}\sum_{l=0}^{j}\beta_{ik}\beta_{jl}X_{skl}\right\}+\ Pu_{iq}u_{jr}\delta_{1t}=0, \tag{9}$$

where $\beta_{ik}=\alpha_{ik}/m$, $\beta_{jl}=\alpha_{jl}/n$, $\alpha_{ik}=1-(\delta_{0k}+\delta_{ik})/2$, $\alpha_{jl}=1-(\delta_{0l}+\delta_{jl})/2$, $t=1$–8, $i=1$–m, $j=1$–n, $u_{iq}=u(\eta_i-\eta_q)$, $u_{jr}=u(\zeta_j-\zeta_r)$.

By retaining the quantities at main point (i,j) on the left-hand side of the equation and putting other quantities on the right-hand side, and using the matrix transition, the solution X_{pij} of the above Eq. (9) is obtained as follows:

$$X_{pij} = \sum_{t=1}^{8}\left\{\sum_{k=0}^{i}\beta_{ik}A_{pt}[X_{tk0} - X_{tkj}(1-\delta_{ik})] + \sum_{l=0}^{j}\beta_{jl}B_{pt}[X_{t0l} - X_{til}(1-\delta_{jl})] + \sum_{k=0}^{i}\sum_{l=0}^{j}\beta_{ik}\beta_{jl}C_{ptkl}X_{tkl}(1-\delta_{ik}\delta_{jl})\right\} - A_{p1}Pu_{iq}u_{jr}, \tag{10}$$

where $p = 1$–8, A_{pt}, B_{pt} and C_{ptkl} are given in Appendix A.

In Eq. (10), the quantity X_{pij} is not only related to the quantities X_{tk0} and X_{t0l} at the boundary-dependent points but also the quantities X_{tkj}, X_{til} and X_{tkl} at the inner-dependent points. The maximal number of the unknown quantities is $6(m-1)(n-1)+3(m+n+1)$. In order to reduce the unknown quantities, the area $[i,j]$ is spread according to the regular order as $[1,1]$, $[1,2]$, …, $[1,n]$, $[2,1]$, $[2,2]$, …, $[2,n]$, …, $[m,1]$, $[m,2]$, …, $[m,n]$. With the spread of the area according to the above-mentioned order, the quantities X_{tkj}, X_{til} and X_{tkl} at the inner-dependent points can be eliminated by substituting the obtained results into the corresponding terms of the right-hand side of Eq. (10). By repeating this process, the quantity X_{pij} at the main point is only related to the quantities X_{rk0} ($r = 1,3,4,6,7,8$) and X_{s0l} ($s = 2,3,5,6,7,8$) at the boundary-dependent points. The maximal number of the unknown quantities is reduced to $3(m+n+1)$. It can be noted the number of the unknown quantities of the present method are fewer than that of the finite element method for the same divisional number $m(\geqslant 3)$ and $n(\geqslant 3)$. Based on the above consideration, Eq. (10) is rewritten as follows:

$$X_{pij} = \sum_{d=1}^{6}\left\{\sum_{f=0}^{i} a_{pijfd}X_{rf0} + \sum_{g=0}^{j} b_{pijgd}X_{s0g}\right\} + \bar{q}_{pij}P, \tag{11}$$

where a_{pijfd}, b_{pijgd} and $\bar{q}_{pij}$ are given in Appendix B.

Eq. (11) gives the discrete solution of the fundamental differential equation (7) of the bending problem of a plate under a concentrated load, and the discrete Green function is chosen as $X_{8ij}/[\bar{P}a/D_0(1-v_{12}v_{21})]$.

4. Boundary conditions of a rectangular plate

The integral constants X_{rf0} and X_{s0g} involved in the discrete solution (11) are all quantities at the discrete points along the edges $\zeta = 0$ ($y = 0$) and $\eta = 0$ ($x = 0$) of the rectangular plate. There are six integral constants at each discrete point. Half of them are self-evident according to the boundary conditions along the edges $\zeta = 0$ and $\eta = 0$ and half of them are needed to determine by the boundary conditions along the edges $\zeta = 1$ and $\eta = 1$.

The boundary conditions along the edges $\zeta = 0$ and 1 are as follows:

$$\begin{aligned} &\theta_y = \theta_x = w = 0 && \text{for a clamped edge,}\\ &M_y = \theta_x = w = 0 && \text{for a simply supported edge,}\\ &Q_y = M_{xy} = M_y && \text{for a free edge.}\end{aligned}$$

The boundary conditions along the edges $\eta = 0$ and 1 are as follows:

$$
\begin{aligned}
&\theta_y = \theta_x = w = 0 && \text{for a clamped edge,}\\
&M_x = \theta_y = w = 0 && \text{for a simply supported edge,}\\
&Q_x = M_{xy} = M_x && \text{for a free edge.}
\end{aligned}
$$

5. Characteristic equation

By applying the Green function $w(x_0, y_0, x, y)/\bar{P}$ which is the displacement at a point (x_0, y_0) of a plate with a concentrated load $\bar{P}$ at a point (x, y), the displacement amplitude $\hat{w}(x_0, y_0)$ at a point (x_0, y_0) of the rectangular plate during the free vibration is given as follows:

$$\hat{w}(x_0, y_0) = \int_0^a \int_0^a \rho h \omega^2 \hat{w}(x, y)[w(x_0, y_0, x, y)/\bar{P}]\,\mathrm{d}x\,\mathrm{d}y, \tag{12}$$

where ρ is the mass density of the plate material.

By using the numerical integration method and the following non-dimensional expressions:

$$\lambda^4 = \frac{\rho_0 h_0 \omega^2 a^4}{D_0(1 - v_{12}v_{21})}, \quad k = 1/(\mu\lambda^4), \quad H(\eta, \zeta) = \frac{\rho(x, y)}{\rho_0}\frac{h(x, y)}{h_0},$$

$$W(\eta, \zeta) = \frac{\hat{w}(x, y)}{a}, \quad G(\eta_0, \zeta_0, \eta, \zeta) = \frac{w(x_0, y_0, x, y)}{a}\frac{D_0(1 - v_{12}v_{21})}{\bar{P}a},$$

where ρ_0 is the standard mass density, the characteristic equation is obtained from Eq. (12) as

$$\begin{vmatrix}
\mathbf{K}_{00} & \mathbf{K}_{01} & \mathbf{K}_{02} & \cdots & \mathbf{K}_{0m}\\
\mathbf{K}_{10} & \mathbf{K}_{11} & \mathbf{K}_{12} & \cdots & \mathbf{K}_{1m}\\
\mathbf{K}_{20} & \mathbf{K}_{21} & \mathbf{K}_{22} & \cdots & \mathbf{K}_{2m}\\
\vdots & \vdots & \vdots & \ddots & \vdots\\
\mathbf{K}_{m0} & \mathbf{K}_{m1} & \mathbf{K}_{m2} & \cdots & \mathbf{K}_{mm}
\end{vmatrix} = \mathbf{0}, \tag{13}$$

where

$$\mathbf{K}_{ij} = \beta_{mj}\begin{bmatrix}
\beta_{n0}H_{j0}G_{i0j0} - k\delta_{ij} & \beta_{n1}H_{j1}G_{i0j1} & \beta_{n2}H_{j2}G_{i0j2} & \cdots & \beta_{nn}H_{jn}G_{i0jn}\\
\beta_{n0}H_{j0}G_{i1j0} & \beta_{n1}H_{j1}G_{i1j1} - k\delta_{ij} & \beta_{n2}H_{j2}G_{i1j2} & \cdots & \beta_{nn}H_{jn}G_{i1jn}\\
\beta_{n0}H_{j0}G_{i2j0} & \beta_{n1}H_{j1}G_{i2j1} & \beta_{n2}H_{j2}G_{i2j2} - k\delta_{ij} & \cdots & \beta_{nn}H_{jn}G_{i2jn}\\
\vdots & \vdots & \vdots & \ddots & \vdots\\
\beta_{n0}H_{j0}G_{inj0} & \beta_{n1}H_{j1}G_{inj1} & \beta_{n2}H_{j2}G_{inj2} & \cdots & \beta_{nn}H_{jn}G_{injn} - k\delta_{ij}
\end{bmatrix}.$$

6. Numerical results

The described method is used to obtain the frequency parameters and mode shapes for orthotropic plate with variable thickness and various boundary conditions. E-glass/epoxy material ($E_1 = 60.7\,\text{GPa}$, $E_2 = 24.8\,\text{GPa}$, $G_{12} = 12.0\,\text{GPa}$, $v_{12} = 0.23$) is used when no properties of material are appointed specially. The thickness functions are chosen as $h = h_0(1 + \alpha x/a)$ and $h = h_0(1 + \alpha x/a)(1 + \beta y/b)$ for variable thickness in one and two directions, respectively. The ratio of the length and thickness $a/h_0 = 100$ is adopted. In all tables and figures, the symbols F, S, and C denote free, simply supported and clamped edges. Four symbols such as SCFC delegate the boundary conditions of the plate, the first indicating the conditions at $x = 0$, the second at $y = 0$, the third at $x = a$ and the fourth at $y = b$.

6.1. Variable thickness in one direction

In order to examine the convergency, numerical calculation is carried out by varying the number of divisions m and n. The lowest six natural frequency parameters of a CSCS orthotropic square plate with variable thickness in one direction ($\alpha = 0.4$) are shown in Fig. 2. It shows a good convergency of the numerical results by the present method. It can be also noticed that convergent results of frequency parameter can be obtained by using Richardson's extrapolation formula for two cases of divisional numbers $m(= n)$ of 12 and 16. By the same method, the suitable number of divisions $m(= n)$ can be determined for the other plates. In this paper, all the convergent values of frequency parameter are obtained by using Richardson's extrapolation formula for two cases of divisional numbers 12 and 16.

To show the accuracy of the present method and to investigate the effects of the boundary conditions, aspect ratios and variable thickness on the frequency parameters, the lowest six

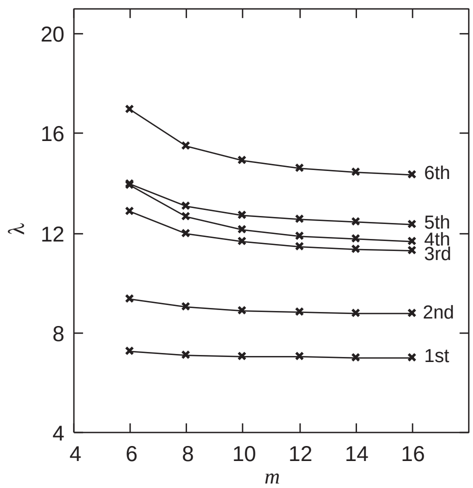

Fig. 2. The natural frequency parameter λ versus the divisional number $m(= n)$ for the CSCS orthotropic square plate with variable thickness in one direction ($\alpha = 0.4$).

Table 1
Natural frequency parameter λ for CSCS and CSSS orthotropic plates with variable thickness in one direction

B.C.	b/a	α	References	Mode sequence number 1st	2nd	3rd	4th	5th	6th
CSCS	0.5	0.0	Ex.*	7.943	11.124	13.268	14.797	14.956	17.666
			Ref. [11]	7.948	11.149	13.287	14.766	15.107	17.754
		0.4	Ex.	8.672	12.141	14.437	16.011	16.472	19.282
			Ref. [11]	8.680	12.172	14.464	16.122	16.519	19.400
		0.8	Ex.	9.307	13.026	15.397	17.346	17.527	20.700
	1.0	0.0	Ex.	6.361	7.941	10.149	10.408	11.125	12.814
			Ref. [11]	6.366	7.948	10.172	10.433	11.149	12.852
		0.4	Ex.	6.945	8.670	11.074	11.350	12.141	13.993
			Ref. [11]	6.952	8.680	11.106	11.382	12.176	14.042
		0.8	Ex.	7.454	9.305	11.874	12.155	13.026	15.026
	2.0	0.0	Ex.	6.036	6.361	6.992	7.905	8.972	9.925
			Ref. [11]	6.041	6.366	7.003	7.948	9.119	9.948
		0.4	Ex.	6.589	6.945	7.635	8.631	9.793	10.830
			Ref. [11]	6.596	6.952	7.649	8.680	9.955	10.861
		0.8	Ex.	7.070	7.454	8.196	9.263	10.504	11.611
CSSS	0.5	0.0	Ex.	7.550	10.429	13.167	13.875	14.762	17.170
			Ref. [11]	7.553	10.444	13.183	13.935	14.788	17.236
		0.4	Ex.	8.276	11.378	14.387	15.127	16.193	18.773
			Ref. [11]	8.281	11.400	14.413	15.199	16.230	18.866
		0.8	Ex.	8.912	12.214	15.370	16.212	17.466	20.198
	1.0	0.0	Ex.	5.572	7.548	9.249	10.221	10.430	12.337
			Ref. [11]	5.574	7.553	9.263	10.246	10.444	12.369
		0.4	Ex.	6.030	8.273	10.050	11.206	11.377	13.507
			Ref. [11]	6.034	8.281	10.068	11.236	11.400	13.548
		0.8	Ex.	6.439	8.905	10.745	12.043	12.223	14.530
	2.0	0.0	Ex.	5.084	5.572	6.415	7.510	8.704	8.968
			Ref. [11]	5.086	5.574	6.425	7.553	8.851	8.981
		0.4	Ex.	5.445	6.030	7.003	8.232	9.634	9.730
			Ref. [11]	5.448	6.034	7.015	8.281	9.713	9.747
		0.8	Ex.	5.761	6.436	7.524	8.865	10.393	10.426

Ex.*: The values obtained by using Richardson's extrapolation formula.

frequency parameters are calculated for 14 kinds of boundary conditions with taper ratios $\alpha = 0.0, 0.4, 0.8$ and aspect ratios $b/a = 0.5, 1.0, 2.0$.

Numerical values for the lowest six natural frequency parameter λ of CSCS, CSSS, SSSS, SSFS, SCSC and SSCS plates are given in Tables 1–3. It can be seen that the frequency parameters

Table 2
Natural frequency parameter λ for SSSS and SSFS orthotropic plates with variable thickness in one direction

B.C.	b/a	α	References	Mode sequence number 1st	2nd	3rd	4th	5th	6th
SSSS	0.5	0.0	Ex.	7.255	9.796	13.087	13.096	14.491	16.716
			Ref. [11]	7.257	9.805	13.103	13.135	14.515	16.764
		0.4	Ex.	7.927	10.709	14.206	14.297	15.860	18.272
			Ref. [11]	7.932	10.719	14.229	14.350	15.896	18.334
		0.8	Ex.	8.524	11.516	15.088	15.351	17.096	19.653
	1.0	0.0	Ex.	4.902	7.253	8.374	9.795	10.079	11.924
			Ref. [11]	4.902	7.256	8.382	9.805	10.103	11.951
		0.4	Ex.	5.360	7.928	9.150	10.703	10.982	13.043
			Ref. [11]	5.362	7.932	9.159	10.719	11.010	13.076
		0.8	Ex.	5.770	8.525	9.831	11.510	11.740	14.048
	2.0	0.0	Ex.	4.190	4.901	5.966	7.214	8.014	8.374
			Ref. [11]	4.191	4.902	5.975	7.257	8.021	8.650
		0.4	Ex.	4.575	5.360	6.526	7.884	8.754	9.148
			Ref. [11]	4.575	5.362	6.637	7.932	8.763	9.159
		0.8	Ex.	4.909	5.771	7.029	8.478	9.402	9.829
SSFS	0.5	0.0	Ex.	6.515	8.126	10.853	12.719	13.608	14.148
			Ref. [11]	6.520	8.133	10.877	12.734	13.628	14.211
		0.4	Ex.	7.292	8.959	11.853	14.137	15.033	15.459
			Ref. [11]	7.316	8.935	11.905	14.147	15.096	15.527
		0.8	Ex.	7.935	9.753	12.714	15.086	16.433	16.611
	1.0	0.0	Ex.	3.533	5.945	6.509	8.129	9.410	9.571
			Ref. [11]	3.528	5.956	6.520	8.133	9.428	9.610
		0.4	Ex.	3.916	6.485	7.310	8.917	10.243	10.712
			Ref. [11]	3.921	6.492	7.316	8.935	10.207	10.761
		0.8	Ex.	4.280	6.967	7.994	9.647	10.982	11.590
	2.0	0.0	Ex.	2.126	3.523	4.994	5.219	5.952	6.474
			Ref. [11]	2.125	3.528	5.002	5.222	5.956	6.520
		0.4	Ex.	2.323	3.918	5.620	5.587	6.482	7.267
			Ref. [11]	2.325	3.921	5.600	5.625	6.492	7.316
		0.8	Ex.	2.519	4.281	5.982	6.120	6.965	7.950

increase with increase of the taper ratio α for the plate with specific boundary condition and aspect ratio b/a, and decrease with the increase of aspect ratio b/a for the plate with the same boundary condition and taper ratio α. The effect of boundary condition on the frequency parameters can be observed by comparing the corresponding results presented in Tables 1 and 2. In these two tables,

Table 3
Natural frequency parameter λ for SCSC and SSCS orthotropic plates with variable thickness in one direction

B.C.	b/a	α	References	Mode sequence number 1st	2nd	3rd	4th	5th	6th
SCSC	0.5	0.0	Ex.	9.885	11.351	13.933	16.025	16.942	17.104
			Ref. [11]	9.897	11.368	13.978	16.077	16.999	17.250
		0.4	Ex.	10.761	12.423	15.220	17.281	18.570	18.666
			Ref. [11]	10.808	12.416	15.262	17.553	18.563	18.814
		0.8	Ex.	11.489	13.397	16.357	18.196	20.004	20.028
	1.0	0.0	Ex.	5.682	8.487	8.617	10.471	11.454	12.238
			Ref. [11]	5.684	8.500	8.625	10.486	11.506	12.276
		0.4	Ex.	6.214	9.262	9.415	11.447	12.451	13.360
			Ref. [11]	6.208	9.281	9.407	11.459	12.562	13.337
		0.8	Ex.	6.692	9.931	10.119	12.324	13.259	14.339
	2.0	0.0	Ex.	4.312	5.239	6.458	7.892	8.043	8.466
			Ref. [11]	4.312	5.243	6.479	7.858	8.052	8.487
		0.4	Ex.	4.709	5.731	7.062	8.505	8.785	9.253
			Ref. [11]	4.704	5.729	7.076	8.580	8.696	9.297
		0.8	Ex.	5.057	6.172	7.601	9.133	9.436	9.945
SSCS	0.5	0.0	Ex.	7.550	10.429	13.167	13.875	14.761	17.171
			Ref. [11]	7.553	10.444	13.183	13.935	14.788	17.236
		0.4	Ex.	8.221	11.401	14.238	15.160	16.097	18.728
			Ref. [11]	8.226	11.424	14.261	15.238	16.135	18.817
		0.8	Ex.	8.813	12.255	15.103	16.276	17.290	20.105
	1.0	0.0	Ex.	5.572	7.548	9.249	10.221	10.428	12.339
			Ref. [11]	5.574	7.553	9.263	10.246	10.444	12.369
		0.4	Ex.	6.147	8.219	10.146	11.082	11.401	13.460
			Ref. [11]	6.151	8.226	10.166	11.111	11.424	13.500
		0.8	Ex.	6.653	8.811	10.927	11.816	12.254	14.455
	2.0	0.0	Ex.	5.084	5.572	6.415	7.510	8.704	8.968
			Ref. [11]	5.086	5.574	6.425	7.553	8.851	8.981
		0.4	Ex.	5.656	6.147	7.021	8.178	9.558	9.849
			Ref. [11]	5.659	6.151	7.033	8.266	9.614	9.869
		0.8	Ex.	6.152	6.653	7.557	8.768	10.436	10.616

the highest frequency parameters can be obtained for CSCS plates, then successively for CSSS, SSSS and SSFS. It shows that with decrease of boundary constraints, which results in decrease of stiffness, frequency parameters decrease significantly. From Tables 1 and 3, it can be found that even for the plates with the same aspect ratio, taper ratio and the same boundary condition, which are two opposite edges clamped and two opposite edges simply supported, the results of CSCS and SCSC orthotropic plates are quite different. For CSCS plate, the longitudinal direction of the orthotropic material is coincident with the simply supported edges, but for SCSC plate, it is coincident with the clamped edges. It shows that the direction of principle material axes also influences the frequency parameters greatly. For the square plates with specific taper ratio, the fundamental frequency of CSCS plate is higher than that of SCSC plate. By comparing the results

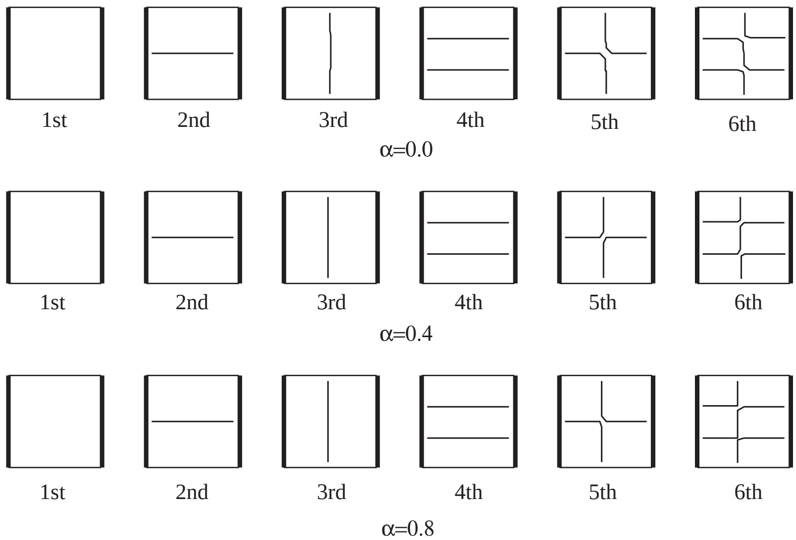

Fig. 3. Nodal patterns for CSCS orthotropic square plates with variable thickness in one direction.

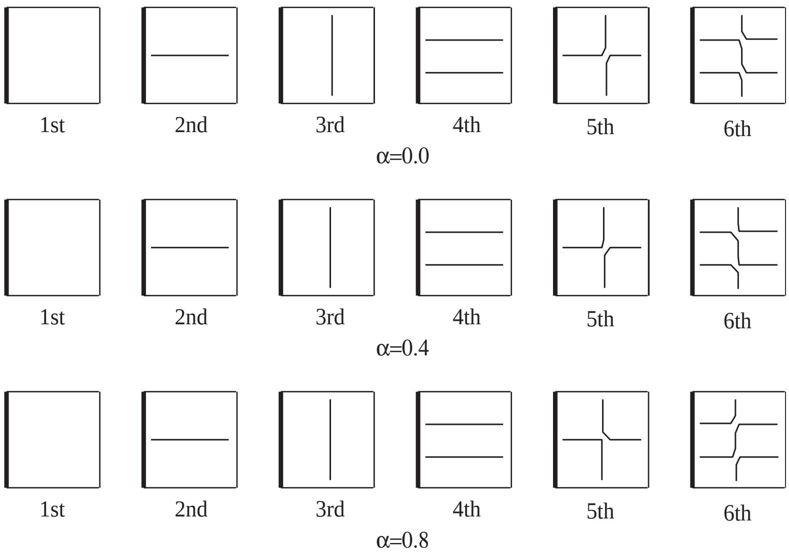

Fig. 4. Nodal patterns for CSSS orthotropic square plates with variable thickness in one direction.

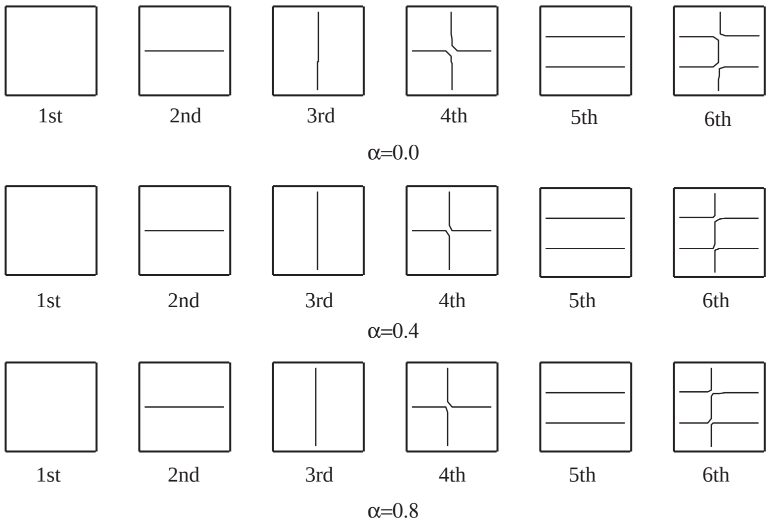

Fig. 5. Nodal patterns for SSSS orthotropic square plates with variable thickness in one direction.

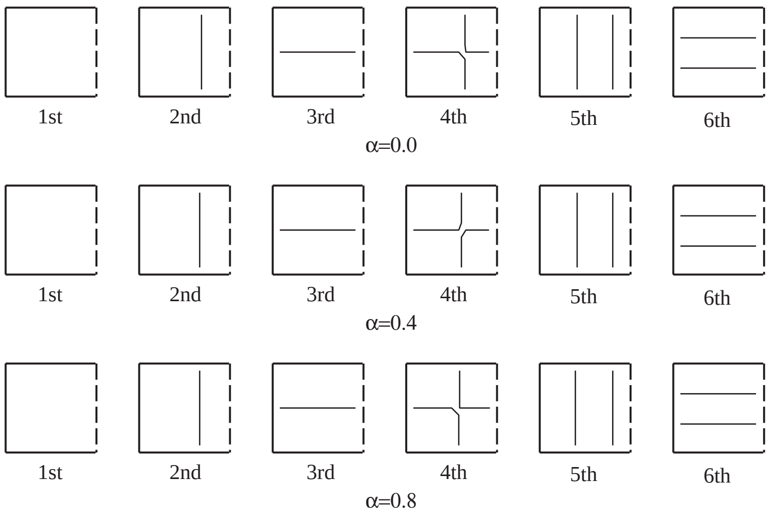

Fig. 6. Nodal patterns for SSFS orthotropic square plates with variable thickness in one direction.

shown in Tables 1 and 3, it can be also noticed that the frequency parameters of CSSS and SSCS plate are the same for the case of uniform thickness ($\alpha = 0.0$), but different for the cases of variable thickness $\alpha = 0.4, 0.8$. The fundamental frequencies of SSCS plates with $\alpha = 0.4, 0.8$ are higher than those of CSSS plates for $b/a = 1, 2$, but lower for $b/a = 0.5$. The results obtained by Bert and Malik [11] are also shown in the above tables. It can be seen that the numerical results of the present method have satisfactory accuracy. The results presented in Tables 1–3 are limited to

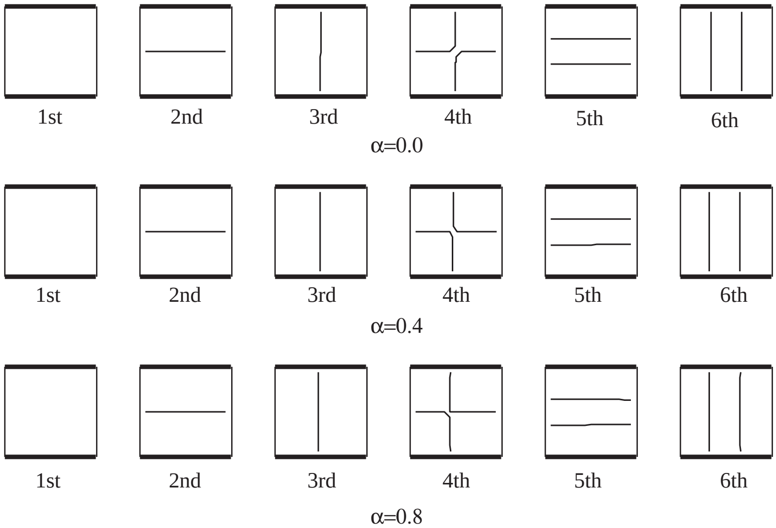

Fig. 7. Nodal patterns for SCSC orthotropic square plates with variable thickness in one direction.

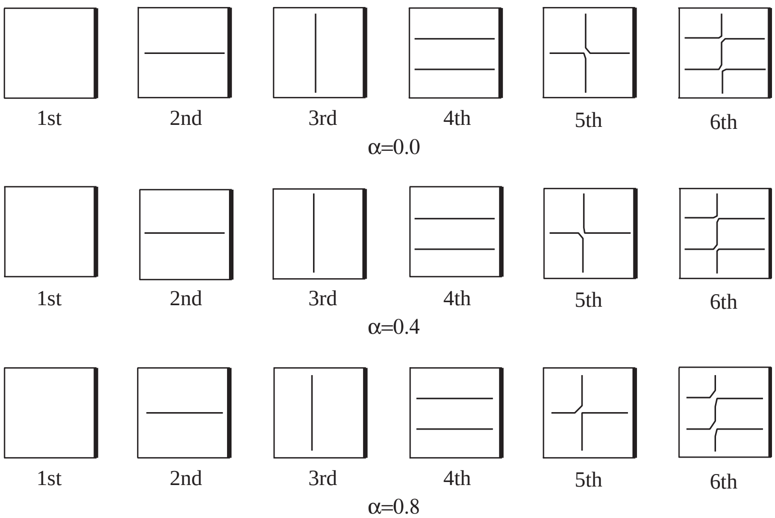

Fig. 8. Nodal patterns for SSCS orthotropic square plates with variable thickness in one direction.

plates with two opposite edges having the same thickness and simply supported boundary conditions.

The nodal patterns of the lowest six modes of the above plates with $b/a = 1$ are shown in Figs. 3–8. With change of the boundary conditions, the orders of some mode shapes change. From Figs. 4 and 8, it is noticed that the vertical nodal lines tend to be close to simply supported edges. In Fig. 6, the vertical nodal lines are close to the free edges. These show the vertical nodal lines have the trend to be close to the edge with less boundary constraint. The trend can be found in the third, fifth and sixth modes in Figs. 4 and 8, and in the second, fourth and fifth modes in

Table 4
Natural frequency parameter λ for CCCC and CCSC orthotropic plates with variable thickness in one direction

B.C.	b/a	α	References	Mode sequence number 1st	2nd	3rd	4th	5th	6th
CCCC	0.5	0.0	Ex.	10.194	12.289	15.301	16.131	17.329	18.632
			Ref. [12]	10.206	12.318	15.393	16.182	17.391	—
		0.4	Ex.	11.113	13.422	16.695	17.476	18.954	20.316
			Ref. [12]	11.132	13.463	16.813	17.546	19.044	—
		0.8	Ex.	11.894	14.419	17.908	18.511	20.397	21.800
	1.0	0.0	Ex.	6.780	8.953	10.293	11.615	11.686	13.636
			Ref. [12]	6.785	8.967	10.317	11.643	11.741	—
		0.4	Ex.	7.402	9.770	11.232	12.679	12.730	14.896
			Ref. [12]	7.410	9.787	11.265	12.719	12.794	—
		0.8	Ex.	7.945	10.475	12.046	13.610	13.602	16.008
	2.0	0.0	Ex.	6.080	6.532	7.320	8.347	9.698	9.941
			Ref. [12]	6.085	6.538	7.342	8.428	9.698	—
		0.4	Ex.	6.638	7.132	7.993	9.112	10.564	10.847
			Ref. [12]	6.644	7.140	8.018	9.202	10.659	—
		0.8	Ex.	7.122	7.654	8.579	9.776	11.630	11.283
CCSC	0.5	0.0	Ex.	10.013	11.783	14.597	16.074	17.121	17.878
			Ref. [12]	11.805	14.662	16.124	17.179	18.067	—
			Ref. [15]	10.035	11.830	14.710	—	—	—
		0.4	Ex.	10.982	12.896	15.928	17.465	18.809	19.474
			Ref. [12]	12.928	16.012	17.535	18.876	19.718	—
		0.8	Ex.	11.796	13.892	17.096	18.509	20.305	20.872
	1.0	0.0	Ex.	6.156	8.683	9.435	11.007	11.555	13.135
			Ref. [12]	6.159	8.695	9.450	11.028	11.608	—
		0.4	Ex.	6.707	9.528	10.260	12.027	12.650	14.298
			Ref. [12]	6.711	9.544	10.280	12.055	12.713	—
		0.8	Ex.	7.196	10.256	10.982	12.929	13.552	15.307
	2.0	0.0	Ex.	5.156	5.816	6.826	8.018	8.988	9.330
			Ref. [12]	5.158	5.821	6.849	8.099	9.003	—
		0.4	Ex.	5.533	6.316	7.468	8.796	9.753	10.141
			Ref. [12]	5.536	6.321	7.493	8.886	9.773	—
		0.8	Ex.	5.863	6.759	8.035	9.474	10.419	10.849

Fig. 6. From Figs. 3–8, it can be noted that with increase of taper ratio, the vertical nodal lines move to the thinner part of the plates. Obvious change can be seen in the third, fifth and sixth modes in Fig. 3, and corresponding modes in other figures.

Table 5
Natural frequency parameter λ for SCFC and FCCC orthotropic plates with variable thickness in one direction

B.C.	b/a	α	References	Mode sequence number 1st	2nd	3rd	4th	5th	6th
SCFC	0.5	0.0	Ex.	9.577	10.335	12.144	14.872	15.790	16.344
			Ref. [12]	9.580	10.332	12.149	14.925	16.399	—
		0.4	Ex.	10.679	11.472	13.320	16.257	17.275	18.246
			Ref. [12]	10.698	11.474	13.336	16.324	17.343	—
		0.8	Ex.	11.466	12.584	14.386	17.465	18.196	19.902
	1.0	0.0	Ex.	4.901	6.486	8.030	9.183	9.615	11.287
			Ref. [12]	4.897	6.483	8.009	9.124	9.617	—
		0.4	Ex.	5.529	7.128	8.976	9.999	10.470	12.480
			Ref. [12]	5.526	7.101	8.999	10.064	10.484	—
		0.8	Ex.	6.065	7.676	9.772	10.971	11.225	13.498
	2.0	0.0	Ex.	2.648	4.171	5.302	5.695	6.180	7.315
			Ref. [12]	2.635	4.172	5.298	5.706	7.252	—
		0.4	Ex.	2.959	4.678	5.720	6.398	6.747	8.031
			Ref. [12]	2.949	4.686	5.715	6.420	8.036	—
		0.8	Ex.	3.249	5.137	6.098	7.096	7.180	8.683
FCCC	0.5	0.0	Ex.	9.601	10.557	12.642	15.635	15.730	16.449
			Ref. [12]	15.632	17.828	22.150	25.098	28.759	—
		0.4	Ex.	10.025	11.454	13.788	16.395	16.986	17.840
			Ref. [12]	16.429	17.088	22.831	24.829	28.933	—
		0.8	Ex.	10.379	12.264	14.815	16.824	18.243	18.978
	1.0	0.0	Ex.	5.017	7.082	8.050	9.443	10.444	11.118
			Ref. [12]	7.068	9.436	10.457	12.186	14.293	—
		0.4	Ex.	5.330	7.793	8.458	10.263	11.477	11.622
			Ref. [12]	7.782	10.258	11.495	13.124	14.861	—
		0.8	Ex.	5.636	8.434	8.820	11.002	12.203	12.209
	2.0	0.0	Ex.	3.058	4.354	5.792	6.154	6.844	7.371
			Ref. [12]	3.042	4.341	5.796	6.154	7.308	—
		0.4	Ex.	3.434	4.687	6.143	6.887	7.553	7.635
			Ref. [12]	3.414	4.663	6.140	6.887	7.538	—
		0.8	Ex.	3.800	5.012	6.479	7.532	8.185	8.002

Tables 4 and 5 present the numerical results for the lowest six natural frequency parameter λ of the CCCC, CCSC, SCFC and FCCC plates with taper ratios $\alpha = 0.0, 0.4, 0.8$ and aspect ratios $b/a = 0.5, 1.0, 2.0$. The results obtained by the present method are compared with those of Ashour [12]. It can be noticed that the present results agree well with Ashour's results for CCCC

Table 6
Natural frequency parameter λ for CCCS, SSSC, SSCC and FFCF orthotropic plates with variable thickness in one direction

B.C.	b/a	α	Mode sequence number 1st	2nd	3rd	4th	5th	6th
CCCS	0.5	0.0	8.958	11.616	14.681	14.943	16.153	18.428
		0.4	9.776	12.681	15.944	16.302	17.660	20.120
		0.8	10.482	13.612	16.950	17.478	19.000	21.613
	1.0	0.0	6.533	8.417	10.211	11.035	11.349	13.207
		0.4	7.133	9.189	11.143	12.029	12.387	14.425
		0.8	7.656	9.857	11.949	12.869	13.293	15.495
	2.0	0.0	6.055	6.438	7.147	8.121	9.803	9.616
		0.4	6.610	7.030	7.804	8.865	10.692	10.491
		0.8	7.092	7.545	8.377	9.513	11.448	11.246
SSSC	0.5	0.0	8.493	10.475	13.454	14.547	15.679	17.019
		0.4	9.269	11.454	14.693	15.742	17.175	18.514
		0.8	9.938	12.330	15.780	16.645	18.514	19.757
	1.0	0.0	5.238	7.855	8.483	10.100	10.756	12.178
		0.4	5.824	8.463	9.195	11.214	11.801	13.360
		0.8	6.164	9.219	9.966	11.865	12.488	14.264
	2.0	0.0	4.243	5.058	6.204	7.533	7.986	8.423
		0.4	4.633	5.532	6.785	8.227	8.727	9.202
		0.8	4.973	5.958	7.306	8.832	9.383	9.887
SSCC	0.5	0.0	8.689	11.009	14.183	14.605	15.897	17.625
		0.4	9.432	12.027	15.658	15.589	17.339	19.241
		0.8	10.079	12.925	16.650	16.633	18.632	20.642
	1.0	0.0	5.818	8.090	9.330	10.695	10.879	12.772
		0.4	6.399	8.795	10.232	11.686	11.785	13.932
		0.8	6.912	9.414	11.017	12.554	12.552	14.961
	2.0	0.0	5.115	5.684	6.612	7.759	8.977	9.287
		0.4	5.687	6.261	7.226	8.442	9.860	10.185
		0.8	6.184	6.770	7.771	9.044	10.626	10.726
FFCF	0.5	0.0	2.344	4.258	5.878	7.862	9.736	9.922
		0.4	2.824	4.905	6.630	8.576	10.394	10.885
		0.8	3.290	5.408	7.271	9.248	10.945	11.771

Table 6 (*continued*)

B.C.	b/a	α	Mode sequence number 1st	2nd	3rd	4th	5th	6th
	1.0	0.0	2.238	3.436	5.348	5.942	6.518	8.178
		0.4	2.850	3.747	5.887	6.644	7.278	8.739
		0.8	3.263	4.248	6.263	7.306	7.883	9.214
	2.0	0.0	2.357	2.709	3.507	4.617	5.884	5.952
		0.4	2.844	3.157	3.934	5.038	6.442	6.570
		0.8	3.275	3.565	4.329	5.432	6.774	7.293

plates. For CCSC plates with $b/a = 1, 2$, they still agree each other, but for plates with $b/a = 0.5$, difference can be found. The difference can also be found in the results for SCFC plates, especially in those for FCCC plates. Due to the lack of the published information on orthotropic plates with variable thickness, no other suitable references can be used for comparison. But comparing the results of CCCC and FCCC shown in Tables 4 and 5, respectively, it is inferred Ashour may have lost some of the lower frequency parameters for FCCC plates. According to the conclusions obtained earlier, the frequencies of FCCC plates should be lower than those corresponding results of CCCC plates. So the fundamental frequency of FCCC plate with $\alpha = 0.4$ and $b/a = 0.5$ is expected to be lower than 11.132 and his results is 16.429. In order to confirm the accuracy of the present method further, the lower three frequency parameters are calculated by using the solution obtained by Hearmon [15] for uniform E-glass/epoxy plates with $b/a = 0.5$. These results are also shown in Table 4. Although the results presented in Tables 4 and 5 are not limited to plates with two opposite edges simply supported, they are still limited to plates with two opposite edges having the same boundary conditions and the same thickness.

As an application of the present method, the numerical results are presented for the plates with general boundary conditions. The number of the combination of the boundary conditions is too large to be considered completely, so the numerical results of the lowest six natural frequency parameter λ are given only for CCCS, SSSC, SSCC and FFCF plates with taper ratios $\alpha = 0.0, 0.4, 0.8$ and aspect ratios $b/a = 0.5, 1.0, 2.0$. These results are shown in Table 6.

6.2. Variable thickness in two directions

As another application of the present method, the numerical results are given for the plates with linearly variable thickness in two directions. Table 7 presents the results for the plates with six kinds of boundary conditions and four kinds of thickness variation. The lowest two frequency parameters versus the aspect ratio are shown in Fig. 9.

At last, the numerical results are given for plates made of isotropic material ($\nu = 0.3$), graphite–epoxy material ($E_1/E_2 = 40.0, G_{12}/E_2 = 0.5, \nu_{12} = 0.25$) and glass–epoxy ($E_1/E_2 =$

Table 7
Natural frequency parameter λ for orthotropic plates with variable thickness in two directions

B.C.	α	β	Mode sequence number 1st	2nd	3rd	4th	5th	6th
CCCC	−0.5	−0.5	4.955	6.548	7.440	8.502	8.533	9.989
	−0.5	0.5	6.453	8.510	9.748	11.070	11.056	13.031
	0.5	−0.5	6.447	8.525	9.671	11.103	11.108	12.993
	0.5	0.5	8.390	11.076	12.666	14.389	14.418	16.887
SSSC	−0.5	−0.5	3.872	5.716	6.252	7.483	7.778	8.786
	−0.5	0.5	5.038	7.499	8.015	9.678	10.148	11.433
	0.5	−0.5	5.016	7.442	8.115	9.717	10.169	11.423
	0.5	0.5	6.536	9.729	10.398	12.580	13.311	14.855
SSSS	−0.5	−0.5	3.635	5.335	6.086	7.221	7.358	8.616
	−0.5	0.5	4.704	6.937	7.966	9.372	9.536	11.425
	0.5	−0.5	4.708	6.933	7.904	9.397	9.590	11.207
	0.5	0.5	6.086	9.022	10.350	12.136	12.439	14.858
SCFC	−0.5	−0.5	3.431	4.815	5.475	6.730	7.064	7.410
	−0.5	0.5	4.467	6.303	6.989	8.628	9.206	9.717
	0.5	−0.5	4.831	6.231	7.879	8.771	9.060	10.936
	0.5	0.5	6.301	8.084	10.235	11.429	11.849	14.200
CCCS	−0.5	−0.5	4.734	6.184	7.258	8.047	8.336	9.706
	−0.5	0.5	6.259	8.009	9.720	10.421	10.891	12.629
	0.5	−0.5	6.158	8.052	9.444	10.522	10.832	12.613
	0.5	0.5	8.137	10.417	12.630	13.605	14.132	16.382
SSCC	−0.5	−0.5	4.248	5.959	6.779	7.875	8.015	9.329
	−0.5	0.5	5.481	7.795	8.715	10.187	10.412	12.198
	0.5	−0.5	5.637	7.653	8.922	10.270	10.274	12.191
	0.5	0.5	7.248	9.991	11.475	13.252	13.359	15.785

4.67, $G_{12}/E_2 = 0.5, v = 0.26$). CFFF and SSSS plates with variable thickness are considered. In Table 8, the results of plates with uniform thickness or variable thickness in one direction are also given and compared with those obtained by Liew et al. [4,16,17] and Lam et al. [18]. These results are in good agreement.

7. Conclusions

A discrete method is extended for analyzing the free vibration problem of orthotropic rectangular plates with variable thickness. The characteristic equation of the

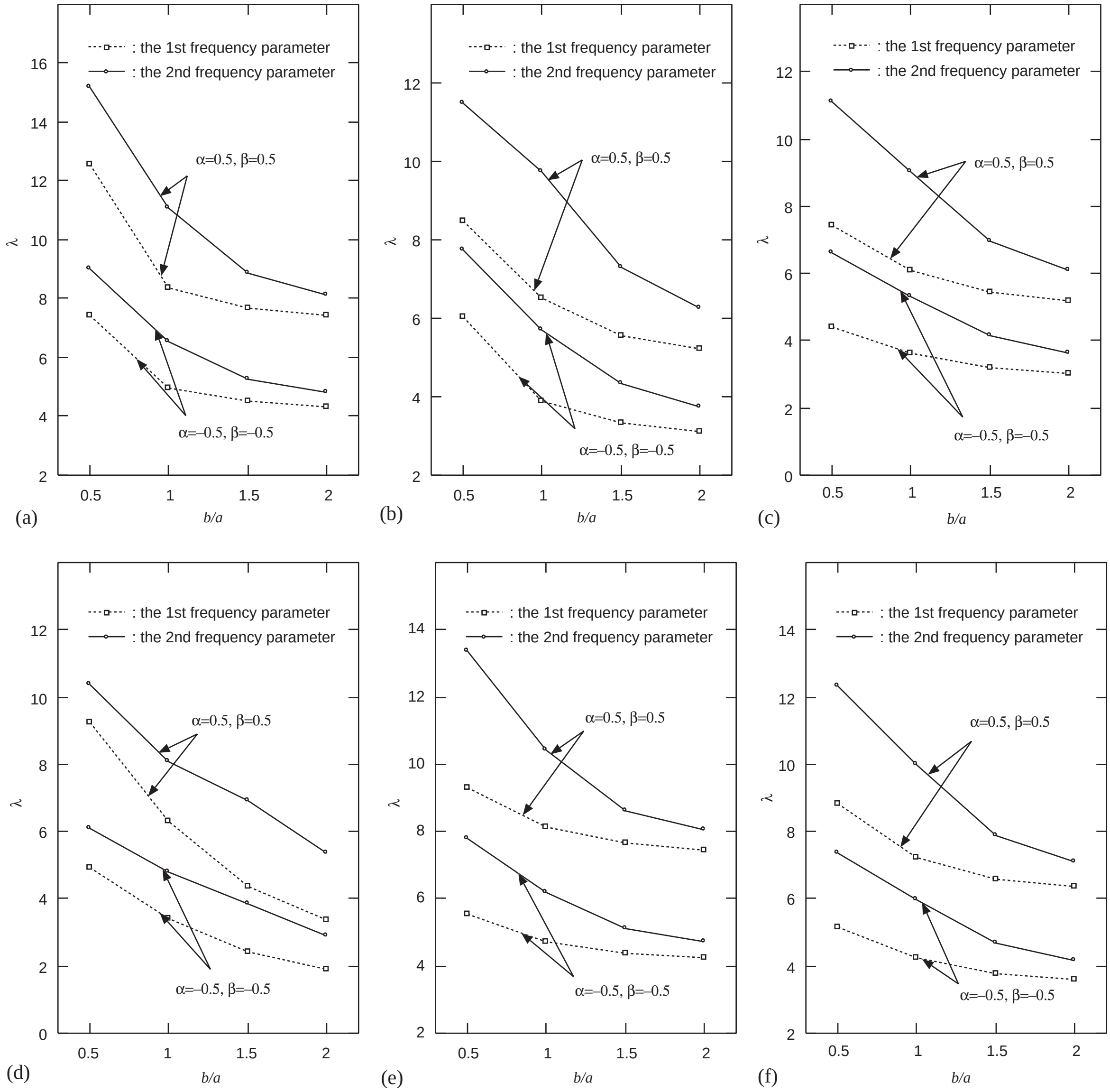

Fig. 9. The natural frequency parameter λ versus the aspect ratio for the orthotropic rectangular plates with variable thickness in two directions. (a) CCCC, (b) SSSC, (c) SSSS, (d) SCFC, (e) CCCS and (f) SSCC.

free vibration is got by using the Green function. The effects of the boundary conditions, aspect ratios and variable thickness in one and two directions on the frequencies are considered. The results by the present method have been compared with those previously reported. It shows that the present results have a good convergence and satisfactory accuracy.

Table 8
Natural frequency parameter λ for isotropic or orthotropic plates with variable thickness

B.C.	Material	b/a	α	β	References	Mode sequence number					
						1st	2nd	3rd	4th	5th	6th
CFFF	Isotropic	0.5	0	0	Present	1.898	3.926	4.738	7.083	7.927	9.869
					Ref. [4]	1.899	3.939	4.740	7.107	7.941	9.849
			−0.4	0	Present	1.955	3.762	4.414	6.299	7.160	8.366
					Ref. [4]	1.955	3.772	4.416	6.315	7.170	8.376
			−0.8	0	Present	2.093	3.524	4.009	5.256	6.100	6.329
					Ref. [4]	2.093	3.530	4.011	5.265	6.093	6.350
			−0.5	−0.5	Present	1.753	3.278	3.802	5.277	5.957	6.841
			−0.5	0.5	Present	2.229	4.176	4.858	6.791	7.727	8.841
			0.5	−0.5	Present	1.650	3.608	4.488	6.795	7.601	9.409
			0.5	0.5	Present	2.098	4.594	5.714	8.782	9.760	12.181
		1.0	0	0	Present	1.908	2.981	4.721	5.335	5.685	7.521
					Ref. [16]	1.91	2.99	4.73	5.34	—	—
			−0.5	−0.5	Present	1.751	2.430	3.633	3.886	4.353	5.477
			−0.5	0.5	Present	2.236	3.124	4.743	5.048	5.567	7.136
			0.5	−0.5	Present	1.654	2.747	4.378	5.210	5.438	7.095
			0.5	0.5	Present	2.105	3.522	5.659	6.730	7.026	9.319
	Graphite–epoxy	0.5	−0.5	−0.5	Present	4.118	4.860	7.092	8.428	9.931	10.722
			−0.5	0.5	Present	5.408	6.120	9.153	11.380	12.611	13.744
			0.5	−0.5	Present	4.007	5.001	9.926	10.197	11.906	13.563
			0.5	0.5	Present	5.160	6.386	12.870	13.486	14.914	17.283
		1.0	0	0	Present	4.716	4.938	6.218	8.463	11.320	11.704
					Ref. [17]	4.717	4.948	6.132	8.486	11.343	11.810
			−0.5	−0.5	Present	3.874	4.548	5.001	6.107	7.808	8.035
			−0.5	0.5	Present	5.235	5.798	6.355	7.900	10.076	11.121
			0.5	−0.5	Present	3.822	4.489	5.828	8.368	9.617	10.945
			0.5	0.5	Present	5.044	5.686	7.506	10.848	13.107	14.261
SSSS	Glass–epoxy	0.5	−0.5	−0.5	Present	5.436	7.883	9.493	10.619	11.017	13.206
			−0.5	0.5	Present	7.100	10.350	12.492	14.361	14.422	17.420
			0.5	−0.5	Present	7.162	10.137	12.401	13.987	14.305	16.862
			0.5	0.5	Present	9.218	13.212	16.147	18.250	18.317	21.871
		1.0	0	0	Present	5.338	7.401	9.573	10.151	10.663	12.431
					Ref. [18]	5.329	—	—	—	—	—
			−0.5	−0.5	Present	3.933	5.476	6.892	7.403	7.913	9.192
			−0.5	0.5	Present	5.095	7.114	9.075	9.626	10.213	11.949
			0.5	−0.5	Present	5.111	7.090	8.949	9.659	10.279	11.923
			0.5	0.5	Present	6.613	9.218	11.778	12.546	13.245	15.463

Acknowledgements

The present study was sponsored by Takahashi Industrial and Economic Research Foundation.

Appendix A

$$
\begin{aligned}
&A_{p1}=\gamma_{p1},\quad A_{p2}=0,\quad A_{p3}=\gamma_{p2},\quad A_{p4}=\gamma_{p3},\quad A_{p5}=0,\\
&A_{p6}=\bar{D}_{12}\gamma_{p4}+\bar{D}_{22}\gamma_{p5}+\bar{D}_{26}\gamma_{p6},\quad A_{p7}=\bar{D}_{16}\gamma_{p06}+\bar{D}_{26}\gamma_{p07}+\bar{D}_{66}\gamma_{p08},\\
&A_{p8}=k(\bar{A}_{44}\gamma_{p7}+\bar{A}_{45}\gamma_{p8}),\quad B_{p1}=0,\quad B_{p2}=\mu\gamma_{p1},\quad B_{p3}=\mu\gamma_{p3},\\
&B_{p4}=0,\quad B_{p5}=\mu\gamma_{p2},\quad B_{p6}=\mu(\bar{D}_{16}\gamma_{p4}+\bar{D}_{26}\gamma_{p5}+\bar{D}_{66}\gamma_{p6}),\\
&B_{p7}=\mu(\bar{D}_{11}\gamma_{p4}+\bar{D}_{12}\gamma_{p5}+\bar{D}_{16}\gamma_{p6}),\quad B_{p8}=\mu k(\bar{A}_{45}\gamma_{p7}+\bar{A}_{55}\gamma_{p8}),\\
&C_{p1kl}=\mu\gamma_{p3}+\mu\overline{DT}_{kl}\gamma_{p7},\quad C_{p2kl}=\mu\gamma_{p2}+\mu\overline{DT}_{kl}\gamma_{p8},\\
&C_{p3kl}=\mu\bar{D}_{kl}\gamma_{p6},\quad C_{p4kl}=\mu\bar{D}_{kl}\gamma_{p7},\quad C_{p5kl}=\mu\bar{D}_{kl}\gamma_{p4},\\
&C_{p6kl}=-\mu k(\bar{A}_{44}\gamma_{p7}+\bar{A}_{45}\gamma_{p8}),\quad C_{p7kl}=-\mu k(\bar{A}_{45}\gamma_{p7}+\bar{A}_{55}\gamma_{p8}),\\
&C_{p8kl}=0,\ [\gamma_{pt}]=[\rho_{tp}]^{-1},\quad \rho_{11}=\beta_{ii},\quad \rho_{12}=\mu\beta_{jj},\quad \rho_{22}=-\mu\beta_{ij},\\
&\rho_{23}=\beta_{ii},\quad \rho_{25}=\mu\beta_{jj},\quad \rho_{31}=-\mu\beta_{ij},\quad \rho_{33}=\mu\beta_{jj},\quad \rho_{34}=\beta_{ii},\quad \rho_{45}=-\mu\beta_{ij}\bar{D}_{ij},\\
&\rho_{46}=\bar{D}_{12}\beta_{ii}+\mu\bar{D}_{16}\beta_{jj},\quad \rho_{47}=\bar{D}_{16}\beta_{ii}+\mu\bar{D}_{11}\beta_{jj},\\
&\rho_{54}=-\mu\beta_{ij}\bar{D}_{ij},\quad \rho_{56}=\bar{D}_{22}\beta_{ii}+\mu\bar{D}_{26}\beta_{jj},\\
&\rho_{57}=\bar{D}_{26}\beta_{ii}+\mu\bar{D}_{12}\beta_{jj},\quad \rho_{63}=-\mu\beta_{ij}\bar{D}_{ij},\\
&\rho_{66}=\bar{D}_{26}\beta_{ii}+\mu\bar{D}_{66}\beta_{jj},\quad \rho_{67}=\bar{D}_{66}\beta_{ii}+\mu\bar{D}_{16}\beta_{jj},\\
&\rho_{71}=-\mu\beta_{ij}\bar{D}_{ij},\quad \rho_{76}=\mu k\bar{A}_{44}\beta_{ij},\\
&\rho_{77}=\mu k\bar{A}_{45}\beta_{ij},\quad \rho_{78}=k(\bar{A}_{44}\beta_{ii}+\mu\bar{A}_{45}\beta_{jj}),\\
&\rho_{82}=-\mu\beta_{ij}\bar{D}_{ij},\quad \rho_{86}=\mu k\bar{A}_{45}\beta_{ij},\\
&\rho_{87}=\mu k\bar{A}_{55}\beta_{ij},\quad \rho_{88}=k(\bar{A}_{45}\beta_{ii}+\mu\bar{A}_{55}\beta_{jj}),\\
&\text{other}\ \rho_{tp}=0.
\end{aligned}
$$

Appendix B

$$
\begin{aligned}
&a_{1i0i1}=a_{3i0i2}=a_{4i0i3}=1,\quad a_{6i0i4}=a_{7i0i5}=a_{8i0i6}=1,\\
&b_{20jj1}=b_{30jj2}=b_{50jj3}=1,\quad b_{60jj4}=b_{70jj5}=b_{80jj6}=1,\quad b_{30002}=0,\\
&a_{pijfd}=\sum_{t=1}^{8}\left\{\sum_{k=0}^{i}\beta_{ik}A_{pt}[a_{tk0fd}-a_{tkjfd}(1-\delta_{ki})]+\sum_{l=0}^{j}\beta_{jl}B_{pt}[a_{t0lfd}-a_{tilfd}(1-\delta_{lj})]\right.\\
&\qquad\left.+\sum_{k=0}^{i}\sum_{l=0}^{j}\beta_{ik}\beta_{jl}C_{ptkl}a_{tklfd}(1-\delta_{ki}\delta_{lj})\right\},
\end{aligned}
$$

$$
\begin{aligned}
b_{pijfd} = {} & \sum_{t=1}^{8}\left\{\sum_{k=0}^{i}\beta_{ik}A_{pt}[b_{tk0gd} - b_{tkjgd}(1-\delta_{ki})] + \sum_{l=0}^{j}\beta_{jl}B_{pt}[b_{t0lgd} - b_{tilgd}(1-\delta_{lj})]\right. \\
& \left. + \sum_{k=0}^{i}\sum_{l=0}^{j}\beta_{ik}\beta_{jl}C_{ptkl}b_{tklgd}(1-\delta_{ki}\delta_{lj})\right\}, \\
\bar{q}_{pij} = {} & \sum_{t=1}^{8}\left\{\sum_{k=0}^{i}\beta_{ik}A_{pt}[\bar{q}_{tk0} - \bar{q}_{tkj}(1-\delta_{ki})] + \sum_{l=0}^{j}\beta_{jl}B_{pt}[\bar{q}_{t0l} - \bar{q}_{til}(1-\delta_{lj})]\right. \\
& \left. + \sum_{k=0}^{i}\sum_{l=0}^{j}\beta_{ik}\beta_{jl}C_{ptkl} - A_{p1}u_{iq}u_{jr}\right\}.
\end{aligned}
$$

References

[1] P.B. Bhat, P.A.A. Laura, R.G. Gutierrez, V.H. Cortinez, H.C. Sanzi, Numerical experiments on the determination of natural frequencies of transverse vibrations of rectangular plates of non-uniform thickness, *Journal of Sound and Vibration* 138 (1990) 205–219.

[2] R.K. Roy, N. Ganesan, Studies on the dynamic behaviour of a square plate with varying thickness, *Journal of Sound and Vibration* 182 (1995) 355–367.

[3] B. Singh, V. Saxena, Transverse vibration of a rectangular plate with bidirectional thickness variation, *Journal of Sound and Vibration* 198 (1996) 51–65.

[4] K.M. Liew, C.M. Lim, M.K. Lim, Transverse vibration of trapezoidal plates of variable thickness: unsymmetric trapezoids, *Journal of Sound and Vibration* 177 (1994) 479–501.

[5] C.W. Lim, K.M. Liew, Effects of boundary constraints and thickness variation on the vibratory response of rectangular plates, *Thin-Walled Structures* 17 (1993) 133–159.

[6] K.M. Liew, T.Y. Ng, S. Kitipornchai, A semi-analytical solution for vibration of rectangular plates with abrupt thickness variation, *Int. J. Solids Structures* 38 (2001) 4937–4954.

[7] A.W. Leissa, Office of Technology Utilization, NASA, *Vibration of Plates* (NASA SP-160). Washington, DC, 1969.

[8] T. Sakata, Natural frequencies of clamped orthotropic rectangular plates with varying thickness, *Journal of Applied Mechanics* 45 (1978) 871–876.

[9] S.K. Malhotra, N. Ganesan, M.A. Veluswami, Vibrations of orthotropic square plates having variable thickness (parabolic variation), *Journal of Sound and Vibration* 119 (1987) 184–188.

[10] D.V. Bambill, C.A. Rossit, P.A.A. Laura, R.E. Rossi, Transverse vibrations of an orthotropic rectangular plate of linearly varying thickness and with a free edge, *Journal of Sound and Vibration* 235 (2000) 530–538.

[11] C.W. Bert, M. Malik, Free vibration analysis of tapered rectangular plates by differential quadrature method: a semi-analytical approach, *Journal of Sound and Vibration* 190 (1996) 41–63.

[12] A.S. Ashour, A semi-analytical solution of the flexural vibration of orthotropic plates of variable thickness, *Journal of Sound and Vibration* 240 (2001) 431–445.

[13] T. Sakiyama, M. Huang, Free vibration analysis of rectangular plates with variable thickness, *Journal of Sound and Vibration* 216 (1998) 379–397.

[14] T. Sakiyama, M. Huang, M. Matsuda, C. Morita, Free vibration of orthotropic square plates with a square hole, *Journal of Sound and Vibration* 259 (2003) 63–80.

[15] R.F.S. Hearmon, The frequency of flexural vibration of rectangular orthotropic plates with clamped or supported edges, *Transactions of the American Society of Mechanical Engineers, Journal of Applied Mechanics* 26 (1959) 537–740.

[16] K.M. Liew, K.Y. Lam, S.T. Chow, Free vibration analysis of rectangular plates using orthogonal plate function, *Computers and Structures* 34 (1990) 79–85.
[17] K.M. Liew, C.W. Lim, Vibratory characteristics of general laminates, I: symmetric trapezoids, *Journal of Sound and Vibration* 183 (1995) 615–642.
[18] K.Y. Lam, K.M. Liew, S.T. Chow, Two-dimensional orthogonal polynomials for vibration of rectangular composite plates, *Composite Structures* 13 (1989) 239–250.